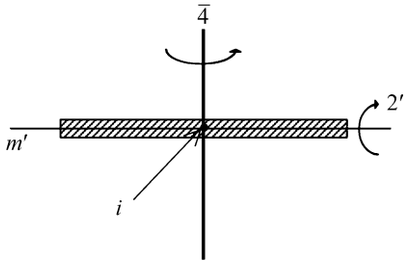

Fig. 2.5.3.1. Four symmetry elements m', i, $2'$ and $\bar{4}$ of an infinitely extended parallel-sided specimen.

Table 2.5.3.1. *Two- and three-dimensional symmetry elements of an infinitely extended parallel-sided specimen*

Symbols in parentheses show CBED symmetries appearing in dark-field patterns.

Two-dimensional symmetry elements	Three-dimensional symmetry elements
1	m' (1_R)
2	i (2_R)
3	$2'$ (m_2, m_R)
4	$\bar{4}$ (4_R)
5	
6	
m	

dimensional symmetry elements. A horizontal mirror plane m', an inversion centre i, a horizontal twofold rotation axis $2'$ and a fourfold rotary inversion $\bar{4}$ are the three-dimensional symmetry elements, and are shown in Fig. 2.5.3.1. The fourfold rotary inversion was not recognized as a symmetry element until the point groups of the diperiodic plane figures were considered (Buxton *et al*., 1976). Table 2.5.3.1 lists these symmetry elements, where the symbols in parentheses express symmetries of CBED patterns expected from three-dimensional symmetry elements.

The diffraction groups are constructed by combining these symmetry elements (Table 2.5.3.2). Two-dimensional symmetry elements and their combinations are given in the top row of the table. The third symmetry m in parentheses is introduced automatically when the first two symmetry elements are combined. Three-dimensional symmetry elements are given in the first column. The equations given below the table indicate that no additional three-dimensional symmetry elements can appear by combination of two symmetry elements in the first column. As a result, 31 diffraction groups are produced by combining the elements in the first column with those in the top row. Diffraction groups in square brackets have already appeared ealier in the table. In the fourth row, three columns have two diffraction groups, which are produced when symmetry elements are combined at different orientations. In the last row, five columns are empty because a fourfold rotary inversion cannot coexist with threefold and sixfold rotation axes. In the last column, the number of independent diffraction groups in each row is given, the sum of the numbers being 31.

2.5.3.2.2. Identification of three-dimensional symmetry elements

It is difficult to imagine the symmetries in CBED patterns generated by the three-dimensional symmetry elements of the sample. The reason is that if a three-dimensional symmetry element is applied to a specimen, it turns it upside down, which is impractical in most experiments. The reciprocity theorem of scattering theory (Pogany & Turner, 1968) enables us to clarify the symmetries of CBED patterns expected from these three-dimensional symmetry elements. A graphical method for obtaining CBED symmetries due to sample symmetry elements is described in the papers of Goodman (1975), Buxton *et al*. (1976) and Tanaka (1989). The CBED symmetries of the three-dimensional symmetries do not appear in the zone-axis patterns, but do in a diffraction disc set at the Bragg condition, each of which we call a dark-field pattern (DP). The CBED symmetries obtained are illustrated in Fig. 2.5.3.2. A horizontal twofold rotation axis $2'$, a horizontal mirror plane m', an inversion centre i and a fourfold rotary inversion $\bar{4}$ produce symmetries m_R (m_2), 1_R, 2_R and 4_R in DPs, respectively.

Next we explain the symbols of the CBED symmetries. (1) Operation m_R is shown in the left-hand part of Fig. 2.5.3.2(*a*), which implies successive operations of (*a*) a mirror m with respect to a twofold rotation axis, transforming an open circle beam (○) in reflection G into a beam (+) in reflection G' and (*b*) rotation R of this beam by π about the centre point of disc G' (or the exact Bragg position of reflection G'), resulting in position ○ in reflection G'. The combination of the two operations is written as m_R. When the twofold rotation axis is parallel to the diffraction vector **G**, two beams (○) in the left-hand part of the figure become one reflection G, and a mirror symmetry, whose mirror line is perpendicular to vector **G** and passes through the centre of disc G, appears between the two beams (the right-hand side figure of Fig. 2.5.3.2*a*). The mirror symmetry is labelled m_2 after the twofold rotation axis. (2) Operation 1_R (Fig. 2.5.3.2*b*) for a horizontal mirror plane is a combination of a rotation by 2π of a beam (○) about a zone axis O (symbol 1), which is equivalent to no rotation, and a rotation by π of the beam about the exact Bragg position or the centre of disc G. (3) Operation 2_R is a rotation by π of a beam (○) in reflection G about a zone axis (symbol 2), which transforms the beam into a beam (+) in reflection $-G$, followed by a rotation by π of the beam (+) about the centre of disc $-G$, resulting in the beam (○) in disc $-G$ (Fig. 2.5.3.2*c*). The symmetry is called translational symmetry after Goodman (1975) because the pattern of disc $+G$ coincides with that of disc $-G$ by a translation. It is emphasized that an inversion centre is identified by the test of translational symmetry about a pair of $\pm G$ dark-field patterns – if one disc can be translated into coincidence with the other, an inversion centre exists. We call the pair ±DP. (4) Operation 4_R (Fig. 2.5.3.2*d*) can be understood in a similar manner. It is noted that regular letters are symmetries about a zone axis, while subscripts R represent symmetries about the exact Bragg position. We call a pattern that contains an exact Bragg position (if possible at the disc centre) a dark-field pattern. As far as CBED symmetries are concerned, we

Table 2.5.3.2. *Symmetry elements of an infinitely extended parallel-sided specimen and diffraction groups*

	1	2	3	4	6	m	$2m(m)$	$3m$	$4m(m)$	$6m(m)$	
1	1	2	3	4	6	m	$2m(m)$	$3m$	$4m(m)$	$6m(m)$	10
(m') 1_R	1_R	21_R	31_R	41_R	61_R	$m1_R$	$2m(m)1_R$	$3m1_R$	$4m(m)1_R$	$6m(m)1_R$	10
(i) 2_R	2_R	[21_R]	6_R	[41_R]	[61_R]	$2_Rm(m_R)$	[$2m(m)1_R$]	$6_Rm(m_R)$	[$4m(m)1_R$]	[$6m(m)1_R$]	4
						[$2_Rm(m_R)$]	[$2m(m)1_R$]	[$3m1_R$]			
($2'$) m_R	m_R	$2m_R(m_R)$	$3m_R$	$4m_R(m_R)$	$6m_R(m_R)$	[$m1_R$]	[$4_Rm(m)m_R$]	[$6_Rm(m_R)$]	[$4m(m)1_R$]	[$6_Rm(m_R)$]	5
($\bar{4}$) 4_R		4_R		[41_R]		$4_Rm(m_R)$	[$4_Rm(m_R)$]		[$4m(m)1_R$]		2

$1_R \times 2_R = 2$, $2_R \times 2_R = 1$, $m_R \times 2_R = m$, $4_R \times 2_R = 4$, $1_R \times m_R = m \times m_R$, $1_R \times 4_R = 4 \times 1_R$, $m_R \times 4_R = m \times 4_R$.

Copyright © 2010 International Union of Crystallography

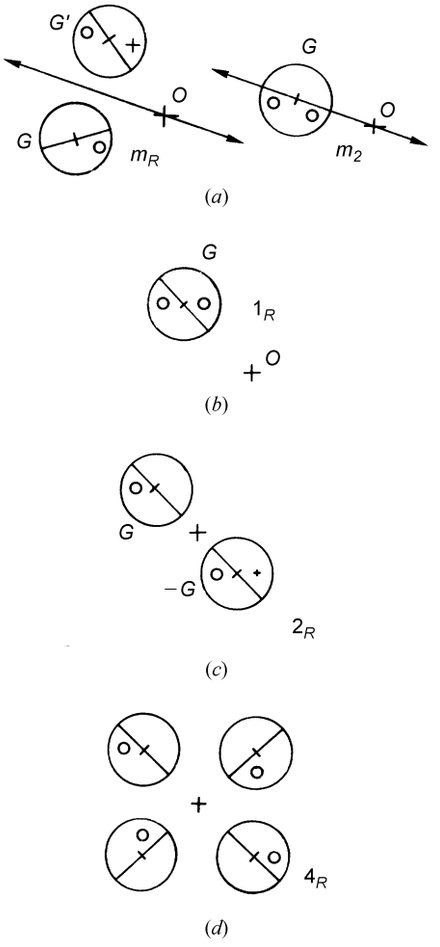

Fig. 2.5.3.2. Illustration of symmetries appearing in dark-field patterns (DPs). (*a*) m_R and m_2; (*b*) 1_R; (*c*) 2_R; (*d*) 4_R, originating from $2'$, m', i and $\bar{4}$, respectively.

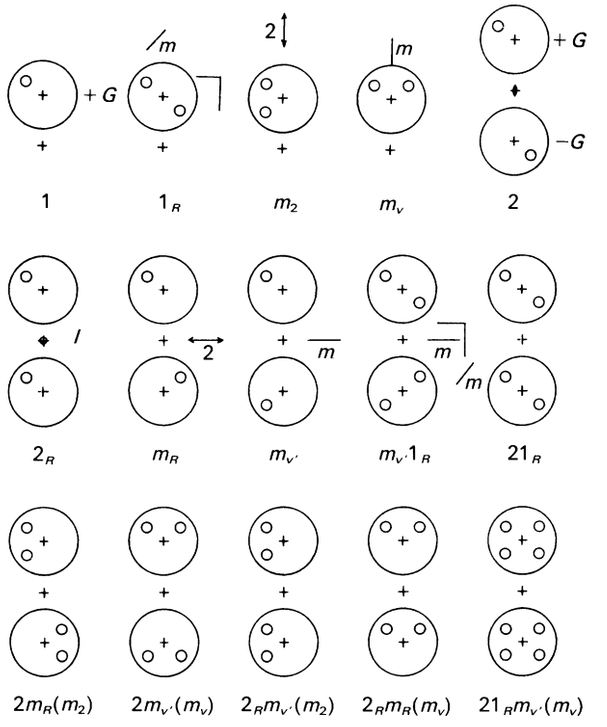

Fig. 2.5.3.3. Illustration of symmetries appearing in dark-field patterns (DPs) and a pair of dark-field patterns (±DP) for the combinations of symmetry elements.

do not use the term dark-field pattern if a disc does not contain the exact Bragg position.

The four three-dimensional symmetry elements are found to produce different symmetries in the DPs. These facts imply that these symmetry elements can be identified unambiguously from the symmetries of CBED patterns.

2.5.3.2.3. Identification of two-dimensional symmetry elements

Two-dimensional symmetry elements that belong to a zone axis exhibit their symmetries in CBED patterns or zone-axis patterns (ZAPs) directly, even if dynamical diffraction takes place. A ZAP contains a bright-field pattern (BP) and a whole pattern (WP). The BP is the pattern appearing in the bright-field disc [the central or 'direct' (000) beam]. The WP is composed of the BP and the pattern formed by the surrounding diffraction discs, which are not exactly excited. The two-dimensional symmetry elements *m*, 1, 2, 3, 4 and 6 yield symmetry m_v and one-, two-, three-, four- and sixfold rotation symmetries, respectively, in WPs, where the suffix *v* for m_v is assigned to distinguish it from mirror symmetry m_2 caused by a horizontal twofold rotation axis.

It should be noted that a BP shows not only the zone-axis symmetry but also three-dimensional symmetries, indicating that the BP can have a higher symmetry than the symmetry of the corresponding WP. The symmetries of the BP due to three-dimensional symmetry elements are obtained by moving the DPs to the zone axis. As a result, the three-dimensional symmetry elements $m', i, 2'$ and $\bar{4}$ produce, respectively, symmetries 1_R, 1, m_2 and 4 in the BP, instead of 1_R, 2_R, m_2 and 4_R in the DPs (Fig. 2.5.3.2). We mention that the BP cannot distinguish whether a specimen crystal has an inversion centre or not, because an inversion centre forms the lowest symmetry 1 in the BP.

In conclusion, all the two-dimensional symmetry elements can be identified from the WP symmetries.

2.5.3.2.4. Diffraction-group determination

All the symmetry elements of the diffraction groups can be identified from the symmetries of a WP and DPs. But it is practical and convenient to use just the four patterns WP, BP, DP and ±DP to determine the diffraction group. The symmetries appearing in these four patterns are given for the 31 diffraction groups in Table 2.5.3.3 (Tanaka, Saito & Sekii, 1983), which is a detailed version of Table 2 of Buxton *et al.* (1976). All the possible symmetries of the DP and ±DP appearing at different crystal orientations are given in the present table. When a BP has a higher symmetry than the corresponding WP, the symmetry elements that produce the BP are given in parentheses in column II except only for the case of 4_R. When two types of vertical mirror planes exist, these are distinguished by symbols m_v and $m_{v'}$. Each of the two or three symmetries given in columns IV and V for many diffraction groups appears in a DP or ±DP in different directions.

It is emphasized again that no two diffraction groups exhibit the same combination of BP, WP, DP and ±DP, which implies that the diffraction groups are uniquely determined from an inspection of these pattern symmetries. Fig. 2.5.3.3 illustrates the symmetries of the DP and ±DP appearing in Table 2.5.3.3, which greatly eases the cumbersome task of determining the symmetries. The first four patterns illustrate the symmetries appearing in a single DP and the others treat those in ±DPs. The pattern symmetries are written beneath the figures. The other symbols are the symmetries of a specimen. The crosses outside the diffraction discs designate the zone axis. The crosses inside the diffraction discs indicate the exact Bragg position.

When the four patterns appearing in three photographs are taken and examined using Table 2.5.3.3 with the aid of Fig. 2.5.3.3, one diffraction group can be selected unambiguously. It is,